

## Proton Spectra from 54.8-MeV Alpha-Particle Reactions: Precompound Emission

A. Chevarier, N. Chevarier, A. Demeyer, G. Hollinger, P. Pertosa, and Tran Minh Duc

*Institut de Physique Nucléaire, Université de Lyon-1, 69621 Villeurbanne, France*

(Received 27 April 1973)

An experimental survey of 54.8-MeV ( $\alpha, p$ ) proton spectra is undertaken for studying pre-equilibrium emission; such deexcitation yields on the average cross sections about 250 mb, the average value measured for all the investigated reactions. Different quantitative formulations are discussed in terms of exciton state mean lifetimes; the exciton and hybrid models are found to give a good interpretation of the proton emission cross sections. A geometrical distinction between the equilibrium and nonequilibrium processes may be attempted. Odd-even effects appear in ( $\alpha, p$ ) reactions by means of partial state density: Odd- $Z$  targets require an initial exciton number  $n_i$  equal to five ( $3p-2n-0h$ ) and even- $Z$  targets equal to four ( $2p-2n-0h$ ). This result may be attributed to a pairing effect according to the odd-even character of residual nuclei.

### I. INTRODUCTION

The statistical theory of the formation and deexcitation of the compound nucleus fails to describe nuclear reactions at excitation energies of some tens of MeV. The discrepancy is due to emission of more high-energy particles than expected from an evaporative process. This emission may be attributed to a direct mechanism in the two-step model<sup>1</sup> used for interpreting high-energy reactions above 100-MeV incident particles. These models associate two completely extreme points of view. The particle emission in the fast step is assumed to occur during the primary binary collisions of the incident nucleon with one or a very few additional nucleons of the target. In the second or slow stage, the emission is treated as the deexcitation of a residual nucleus, in a complete internal equilibrium and where the excitation energy is shared among all nucleons. The attainment of the statistical equilibrium which takes place between these two extreme phases is generally neglected; such an assumption has been shown to be valid.<sup>2</sup>

Recently, a slightly different approach for medium energy reactions initiated by Griffin<sup>3</sup> has been proposed. The model considers the formation of the compound nucleus and the emission of particles during the establishment of the statistical equilibrium.<sup>4</sup> The compound nucleus can be obtained only by absorption of the incident particle through a sequence of intermediate precompound nuclear states. Transitions among these states are assumed to proceed by successive binary interactions creating a particle-hole pair, the excitons, in a single-particle nuclear model. Each of these particle-hole intermediate states may decay by emitting one of the particles, or it may decay by a new residual interaction into another particle-

hole configuration and so on, up to the compound states which are linear combinations of numerous states with a high exciton number. In order to monitor the particle escape from the pre-equilibrium states, it is assumed that all transitions which take place are governed by phase space available for these transitions, i.e., by the density of exciton states  $\rho(E, n)$ : These functions count the different ways in which the excitation energy  $E$  may be partitioned among  $n$  excitons.

From the theorem of detailed balance, Cline and Blann<sup>5</sup> derive the probability of particle emission at each exciton state which can be written for proton emission as

$$W_n^P(\epsilon) d\epsilon = \frac{2s+1}{\pi^2 \hbar^3} m \epsilon \sigma_{\text{inv}}(\epsilon) \frac{\rho(U, \pi_p - 1, \pi_n, \nu_p, \nu_n)}{\rho(E, \pi_p, \pi_n, \nu_p, \nu_n)} d\epsilon, \quad (1)$$

where  $(2s+1)$  accounts for spin degeneracy,  $m$  and  $\epsilon$  are the reduced mass and kinetic energy of the emitted proton, and  $\sigma_{\text{inv}}(\epsilon)$  is the inverse cross section for the absorption by the residual nucleus of a proton with an energy  $\epsilon$ .  $\rho(E, \pi_p, \pi_n, \nu_p, \nu_n)$  and  $\rho(U, \pi_p - 1, \pi_n, \nu_p, \nu_n)$  are the exciton state densities, respectively, for the initial nucleus at excitation energy  $E$  and for the residual nucleus left at energy  $U$  after one proton emission. The exciton state density is written for two types of fermions:  $\pi_p$  and  $\pi_n$  are the numbers of protons and neutrons above Fermi level;  $\nu_p$  and  $\nu_n$  are the number of proton and neutron holes.

The emission of a particle from an  $n$  exciton state can occur only during the mean lifetime of this state  $\tau_n$ . In addition, the probability of populating a particular intermediate state is not equal to one but is depleted by previous emission to  $p(n, E) < 1$ . Therefore the absolute emission from

a precompound state is

$$P_n^p(\epsilon)d\epsilon = p(n, E)W_n^p(\epsilon)\tau_n d\epsilon. \quad (2)$$

Two different approaches have been adopted for evaluating  $\tau_n$ . As pointed out previously, an intermediate state may decay by emitting particles or by decaying to an  $n+2$  exciton state with a two-body interaction creating one additional particle-hole pair. One has to neglect the probability for transitions leading configurations where the exciton number decreases to  $n-2$  or stays unchanged.<sup>6</sup>

$\tau_n$  may be defined rather as the mean time during which the particle of kinetic energy  $\epsilon$  to be emitted can be considered as one of the  $n$  excitons of the precompound state. It is only during this time that the particle emission is governed by the phase space specified in the expression (1) where one proton possesses an energy  $\epsilon$  and the other excitons share the residual energy. So  $\tau_n$  is expressed as<sup>7</sup>

$$\tau_n = \frac{1}{\lambda_c(\epsilon) + \lambda_{n+2}(\epsilon)}, \quad (3)$$

where  $\lambda_c(\epsilon)$  is, as stated by Blann,<sup>7</sup> the escape probability of the nucleon with the energy  $\epsilon$ , and  $\lambda_{n+2}(\epsilon)$  is the complementary probability that this nucleon may collide with a nucleon of the target and given an  $(n+2)$  state. The probability  $\lambda_c(\epsilon)$  can be written out from the law of detailed balance<sup>8</sup>

$$\lambda_c(\epsilon) = \frac{(2s+1)\sigma_{inv} m \epsilon}{\pi^2 \hbar^3 g_p}, \quad (4)$$

where  $g_p$  is the density of states inside the nucleus of the considered nucleon; with an energy  $\epsilon$ , it is taken equal to  $\frac{1}{2}g$ .

It was proposed by Blann<sup>7</sup> that  $\lambda_{n+2}(\epsilon)$  be expressed as the ratio of the velocity of the nucleon to its mean free path  $\Lambda(\epsilon)$  in the nuclear matter:

$$\lambda_{n+2}(\epsilon) = \frac{(2\epsilon/m)^{1/2}}{\Lambda(\epsilon)}. \quad (5)$$

From the above relations, the proton spectrum is given by the following expression given by Blann<sup>7</sup> and Harp and Miller<sup>6</sup> with a different derivation:

$$P_n^p(\epsilon) = p(n, E) \frac{\rho(U, \pi_p - 1, \pi_n, \nu_p, \nu_n)}{\rho(E, \pi_p, \pi_n, \nu_p, \nu_n)} \frac{1}{2} g \frac{\lambda_c(\epsilon)}{\lambda_c(\epsilon) + \lambda_{n+2}(\epsilon)}. \quad (6)$$

In this expression referred to as hybrid model,  $\tau_n$  is dependent only on the energy of the particle and is quite independent of the  $n$  exciton number and independent also of the excitation energy. From another point of view closer to the statisti-

cal theory, the mean lifetime  $\tau_n$  must account for all the competing emissions and internal transitions which participate in the decaying of the  $n$  exciton state. This formulation, referred to as exciton model,<sup>9</sup> expresses  $\tau_n$  as

$$\tau_n = \frac{1}{\lambda_c(E, n) + \lambda_{n+2}(E, n)},$$

where, following Gadioli,<sup>9,10</sup>  $\lambda_c(E, n)$  is defined quite differently than previously as the sum over all particle emissions, mainly neutrons and protons:

$$\lambda_c(E, n) = \sum_{\substack{i=\text{neutron,} \\ \text{proton}}} \int_0^{E-B_i} W_n^i(\epsilon) d\epsilon. \quad (7)$$

$\lambda_{n+2}(E, n)$  is the probability of transition from  $n$  exciton state to  $(n+2)$  state. As the matrix elements responsible for the transitions are unknown,<sup>6</sup> the different empirical approaches<sup>5, 8, 9, 11</sup> are based upon nucleon-nucleon scattering cross sections inside the nuclear matter similar to the hybrid model.

The pre-equilibrium model has been employed for analysis of both excitation functions and particle spectra.<sup>12</sup> The purpose of this paper is to investigate the different theoretical formulations analyzing spectral data which are still scarcely found in the literature. The selected experiment, a survey of 54.8-MeV ( $\alpha, p$ ) reactions, is especially indicated since no data are available except for a single result at 59 MeV,<sup>13</sup> which extends the analyses performed by Griffin,<sup>14</sup> Cline and Blann,<sup>5</sup> and Blann and Mignerey<sup>15</sup> of results at 30 and 42 MeV<sup>16,17</sup> with the pre-equilibrium model.

## II. EXPERIMENTAL PROCEDURE

The experiments were performed on the Lyon University synchrocyclotron with 54.8-MeV  $\alpha$  particles impinging on self-supported foils of <sup>51</sup>V, <sup>54,56,57</sup>Fe, <sup>59</sup>Co, <sup>nat</sup>Cu, <sup>66</sup>Zn, <sup>93</sup>Nb, <sup>nat</sup>Ag, <sup>115</sup>In, <sup>181</sup>Ta, and <sup>197</sup>Au. The thickness of the targets varies from 3 to 10 mg/cm<sup>2</sup>. Beam intensity is 5 nA on the average. The protons are detected by Si detectors. In order to stop 45-MeV protons completely, a thickness greater than 10 mm is required, so we have used a transverse field 15-mm-thick Si-Li junction<sup>18</sup> mounted on a rotatable arm and cooled by a liquid nitrogen cryostat. To identify the proton among the other charged particles, the method of Goulding *et al.*<sup>19</sup> has been employed. The domain of emission energy that the reported experiments intend to cover extends from 5 MeV, the evaporation region, to 45 MeV, the maximum proton energy to be detected. Consequently, a classical two-detector telescope cannot cover this whole energy range with a good

identification,<sup>17</sup> so it was necessary to use a three-detector telescope. The first two detectors are transmission surface barrier Si, and typically 100 and 1000  $\mu\text{m}$  thick; disposed in front of the 15-mm detector they are thermally isolated from it. The final resolution of the telescope attains 200 keV. The low-energy protons are analyzed by the first two detectors, since they do not reach the last one. The higher-energy protons are detected by the entire telescope: The two signals delivered by the transmission junctions are added to supply the energy loss  $\Delta E$  information. The electronic system for the treatment and selection of the proton signals is described elsewhere.<sup>20</sup> With this procedure, the energy loss information  $\Delta E$  is always large enough, around 10% of the total energy of the particle, and the condition for obtaining a good identification signal is fulfilled for the whole proton energy distribution. Therefore it was possible to record the spectrum in a single measurement. A sample of measurements is shown in Fig. 1 for  $^{93}\text{Nb}$  as a target.

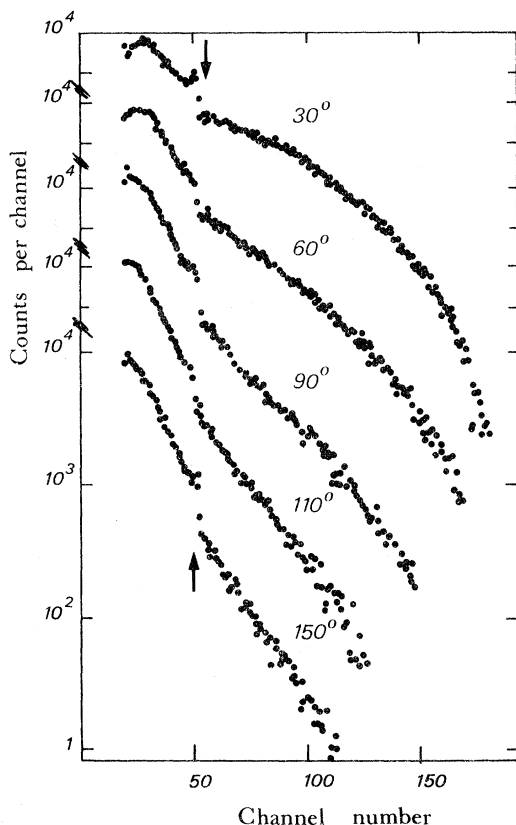


FIG. 1. The differential experimental spectra for the  $^{93}\text{Nb}(\alpha, p)$  reaction at several angles. The arrows indicate the connection of the spectra collected with two and three detectors, respectively.

The data are then corrected for energy absorption in the target and expressed in the center-of-mass system. When running the experiments, contaminations with light elements are carefully avoided because of their high  $(\alpha, p)$  cross sections. This problem has been discussed at length by West.<sup>17</sup> We have made a few measurements, at the same incident energy of 42 MeV as West's experiments, and no disagreement was seen between the two different sets of values.<sup>21</sup> Finally, the errors affecting the absolute value for the cross sections are estimated to be lower than 30%.

### III. DATA REDUCTION

The differential cross sections for proton emission, as indicated in Fig. 2 concerning reactions with  $^{59}\text{Co}$  and  $^{181}\text{Ta}$ , have been accumulated at angles from 20 to 150°, at 15° intervals forward and 30° intervals backward. From the angular distribution obtained with these data, the integration over all angles yields the total absolute spectrum; these results will appear in Fig. 11.

In Fig. 3 spectra at three selected angles, 30, 90 and 150°, are presented for several targets

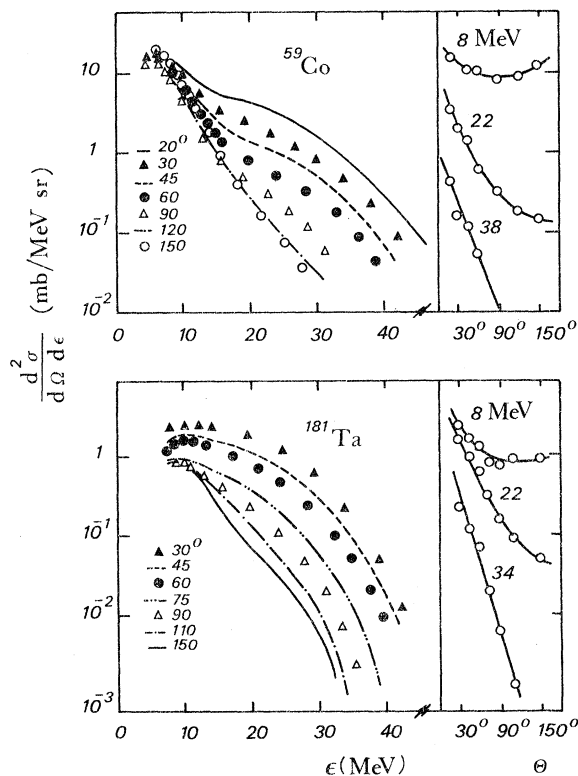


FIG. 2. The differential cross sections for the  $^{59}\text{Co}$  and  $^{181}\text{Ta}(\alpha, p)$  reactions with angular distributions for three kinetic energy regions.

with  $A$  values covering the mass table. For any of the studied reactions no peculiar structure is noticeable in the energy spectrum or in the angular distribution energy. The common behavior can be characterized by a variation of emission cross section with a wide maximum near the Coulomb barrier and then decaying nearly exponentially and monotonously toward high energy. This description is not true for heavy-mass targets where the evaporation peak is very depressed. Indeed, this low-energy portion of spectra classically exhibits every feature of a compound-nucleus process: an angular distribution, flat or rather symmetrical around  $90^\circ$ , and cross sections decreasing with increasing mass values.

On the other side, toward larger energy, the angular distribution is peaked forward with no marked  $A$  dependence of the cross section. Actually the spectra are almost parallel and nearly merged for most of the reactions. These features may be understood intuitively with a fast mechanism in which a small number of nucleons, identical for any target, participates in sharing the excitation energy, the remaining nucleons forming an inert core.

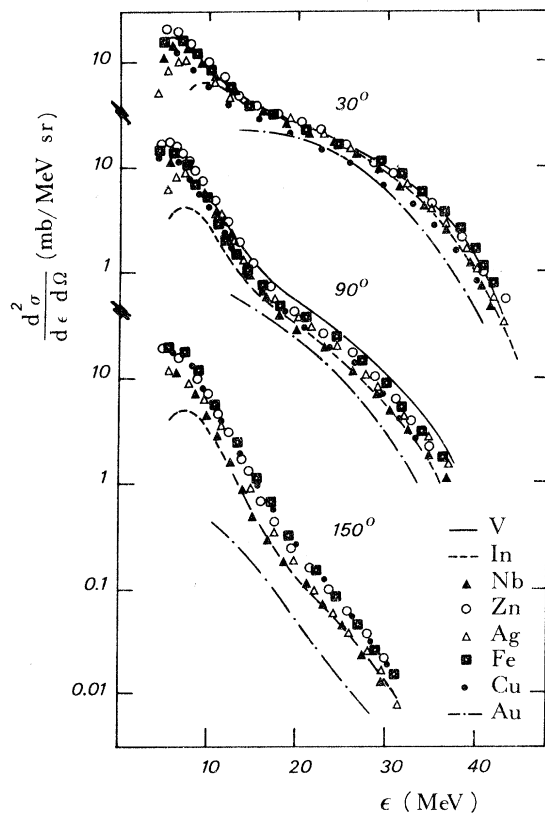


FIG. 3. The differential cross sections at 30, 90, and  $150^\circ$  angles for  $(\alpha, p)$  reactions with different targets along the mass table.

As for the intermediate kinetic energy region, the angular distribution, while still remaining peaked forward, rises at backward angles and it may appear to be flat for angles greater than  $120^\circ$ . This trend leads several authors<sup>16,22,23</sup> to attribute the whole emission at very large angles,  $150^\circ$ , to the evaporation process. However, the values of the level density parameter  $a$  extracted from such analyses are found to be very low and above all, independent of mass number, but they decrease with the excitation energy. These conclusions are quite inconsistent with the Fermi-gas model. Another more realistic point of view<sup>17</sup> is to consider that these misleading conclusions are caused by particles emitted in excess of the cross section predicted by the statistical theory. So, some pre-equilibrium emission has to be taken into consideration. In evaporation calculations we are led to use level density parameter values extracted from analyses of low-energy reaction and classically equal to  $\frac{1}{2}A$ . Proceeding in this manner, we have fitted the calculated compound-nucleus emission shape with the experimental rear-angle spectrum. The normalization region is clearly the low-energy portion of the spectra; the high-energy part which is not interpreted will be attributed to noncompound processes (Fig. 4). We have thus obtained from the total integrated spectrum approximate values of cross sections for the compound and the so-called precompound interactions (Table I). It can be noticed that nonequilibrium processes are increased by a factor of 2 or 3 when the incident energy of  $\alpha$  particles increases from 42 to 54.8 MeV. This fact fully justifies the reported experiments and furnishes a good experimental test of the pre-equilibrium

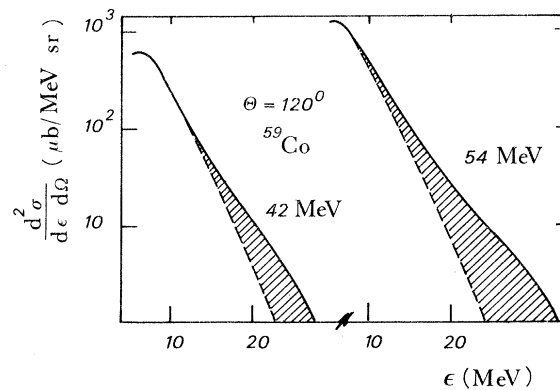


FIG. 4. The  $120^\circ$  cross sections for  $^{59}\text{Co}(\alpha, p)$  spectrum at 42- and 54.8-MeV bombarding energies: The dashed lines are evaporation spectrum shapes calculated with  $a = 7.9 \text{ MeV}^{-1}$  and fitted with experimental data at the lowest-energy region of emission. The hatched part is due to noncompound events.

theory. Figure 5(a) shows indeed that at 54.8 MeV the proton energy spectrum covers a wider range than data with lower incident energies, so the confrontation with theoretical predictions is more compelling. Moreover, the experimental data for precompound emission are also extracted more precisely. As explained in Fig. 5(b), where the spectra are plotted against residual energy calculated for emission of the first proton, the interference with the equilibrium process is much more appreciable for lower incident energies.

#### IV. ANALYSIS AND DISCUSSION

In the expression for the probability of precompound emission, two factors play a fundamental part. The first parameter to be specified is the exciton state density. The basic assumption of precompound formalism is that the initial excitation energy is shared only among a small number of degrees of freedom, the excitons, and, hence, the statistics of partition and particle emission are governed by the particle-hole state density. Secondly, as discussed in Sec. I, the importance of the transition rates between intermediate states has been pointed out in relating the mean lifetimes of these states in order to obtain absolute values of the cross sections.

##### A. Partial State Density

As will be stated quantitatively later, the de-excitation of the first intermediate state, characterized by the exciton number  $n_1$ , from which the particle emission may occur, makes the most important contribution. So it can be recalled from expressions (1) and (2) that the shape of the proton pre-equilibrium spectrum is then proportional to the density of the particular  $(n_1 - 1)$  state

$\rho(\pi_p - 1, \pi_n, \nu_p, \nu_n, U)$  according to

$$\frac{d\sigma}{d\epsilon} \propto \rho(\pi_p - 1, \pi_n, \nu_p, \nu_n, U) \epsilon \sigma_{\text{inv}T_n}.$$

Two different procedures for conducting the analysis can be followed: One is to fix *a priori* the initial exciton number  $n_1$  from arguments concerning the reaction mechanisms,<sup>14,15,24</sup> the other method, which we shall adopt, is to extract this parameter from the spectral data.

The partial state density for a uniform-spacing model of two fermion gases is given by<sup>25</sup>

$$\rho(\pi_p, \pi_n, \nu_p, \nu_n, E) = g_p^{\pi_p} g_n^{\pi_n} \frac{E^{n-1}}{\pi_p! \pi_n! \nu_p! \nu_n! (n-1)!}, \quad (8)$$

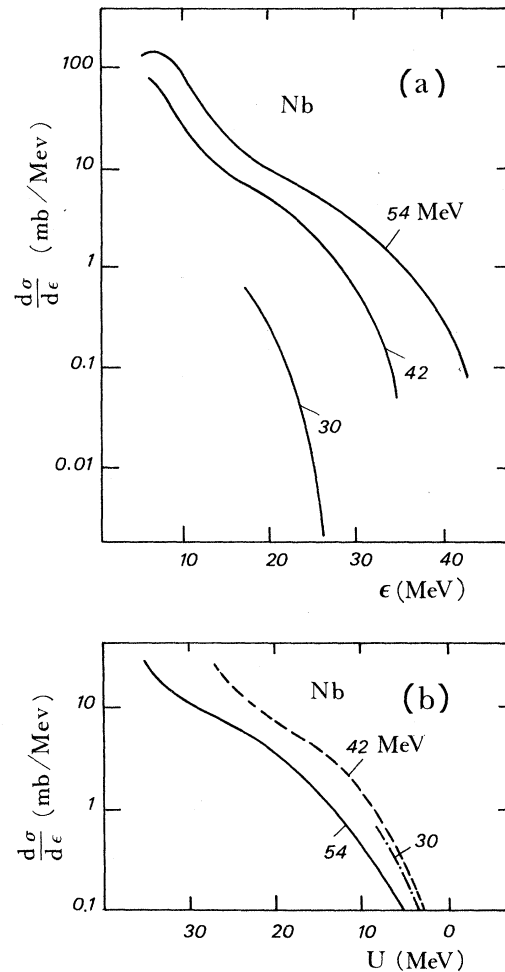


TABLE I. Integrated cross sections for compound and noncompound processes in proton emission with 54- and 42-MeV  $\alpha$ -particle reactions.

Target nuclei	54 MeV		42 MeV	
	Compound cross section (mb)	Precompound cross section (mb)	Compound cross section (mb)	Precompound cross section (mb)
$^{51}\text{V}$	1050	275		
$^{56}\text{Fe}$	1265	235		
$^{58}\text{Co}$	980	220	881 <sup>a</sup>	89 <sup>a</sup> 90 <sup>b</sup>
$^{66}\text{Zn}$	1190	230		
$^{93}\text{Nb}$	700	240	335	85
$^{\text{nat}}\text{Ag}$	500	250		
$^{116}\text{Sn}$	650	255	315	125

<sup>a</sup> See Ref. 17.

<sup>b</sup> See Ref. 21.

FIG. 5. Integrated cross sections for  $^{93}\text{Nb}(\alpha, p)$  reactions at different bombarding energies. Data at 30 MeV are due to Swenson and Gruhn (Ref. 16), 42 MeV due to West (Ref. 17). Spectra in (a) are plotted against kinetic energy of protons and in (b) against residual energy  $U = E - \epsilon - B_p$ .

where  $g_p$  and  $g_n$  are constant single-particle level density of the proton gas and neutron gas, taken both equal to  $\frac{1}{2}g$ .

It is easily seen by means of the above relations that the spectrum shape is a function of  $U^{n_i-2}$ , so the plot of the logarithm of  $(d\sigma/d\epsilon)/\epsilon\sigma_{\text{inv}}\tau_n$  versus the logarithm of  $U$  is linear with a slope equal to  $n_i - 2$ .

In this analysis we first have to examine the expression of the residual energy:  $U = E - B_p - \epsilon$ .  $B_p$  is the proton binding energy. For the level density calculations in the statistical model one usually adds a correcting term according to the odd-even character of the nucleus. Then, as some authors<sup>26</sup> propose, the question of correcting the energy for pairing effects in the exciton state density expression can be examined. As pre-compound emissions populate low-energy residual states, this problem may be of some importance.

A second correction is due to the Pauli principle which tends to reduce the exciton state density;

Williams proposes to shift the energy by a negative term<sup>25</sup>:

$$B = \frac{1}{4} \left( \frac{\pi_p^2 + \nu_p^2 + \pi_p - \nu_p}{g_p} + \frac{\pi_n^2 + \nu_n^2 + \pi_n - \nu_n}{g_n} \right) - \frac{1}{2} \left( \frac{\nu_p}{g_p} + \frac{\nu_n}{g_n} \right).$$

In  $(\alpha, p)$  reactions,  $n_i$  seems to describe 4p-0h or 5p-0h configurations, i.e., with  $\pi_p = 2$  or 3,  $\pi_n = 2$ , and  $\nu_p = \nu_n = 0$ , so with  $g_p = g_n = A/26.6$ ; these factors  $B$  are typically equal (in MeV) to  $78/A$  or  $120/A$ .

Therefore, we have expressed the residual energy without correction, then with an exclusion principle correction and with a pairing term. We have also used the different expressions of the mean lifetime:  $\tau_n$  constant with  $\epsilon$  following Williams<sup>6</sup> or exciton formulation<sup>9,10</sup> or varying with  $\epsilon$  in the hybrid model.<sup>7</sup> A third method derived from a direct mechanism point of view according to Griffin<sup>14</sup> has also been used by plotting  $(d\sigma/d\epsilon)/\epsilon^{1/2}$ .

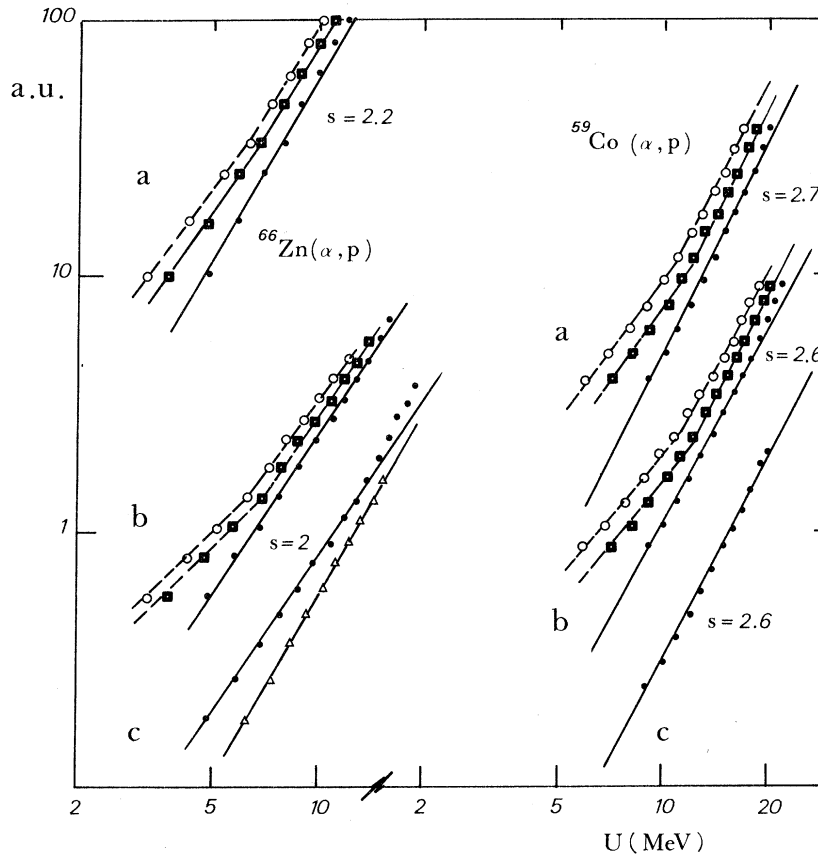


FIG. 6. Different plots for the determination of the initial configuration number  $n_i$  in the  $^{66}\text{Zn}(\alpha, p)$  and  $^{59}\text{Co}(\alpha, p)$  reactions. The curves correspond to the exciton or Williams formulation, b to the hybrid model, and c to the Griffin expression. The symbols are as follows:  $\bullet$ : denotes plots for uncorrected  $U$ ;  $\blacksquare$ : for Pauli-principle-shifted  $U$ ;  $\circ$ : for pairing-shifted  $U$ ; and  $\triangle$ : for back-shifted  $U$ . The angle of emission is  $30^\circ$ . The parameters  $s$  are the slope values obtained from the analysis with unshifted energies.

Figure 6 displays plots from  $^{59}\text{Co}(\alpha, p)^{62}\text{Ni}$  and  $^{66}\text{Zn}(\alpha, p)^{69}\text{Ga}$  spectra at a  $30^\circ$  angle. As emphasized by the results, when the exciton state density expression from the constant spacing model is used the analysis seems to be more satisfactory with the uncorrected residual energy. In this case indeed, the expected linearity extends from the lowest excitation energies up to about 20 MeV, where contributions from higher exciton states appear significant. With shifted energy, especially by pairing effect, the departure of the plot from a single straight line is obvious and the analysis gives two slopes [the residual nuclei selected in this example are even-even ( $^{62}\text{Ni}$ ), so  $\delta = 3.0$  MeV and odd-even ( $^{69}\text{Ga}$ ) so  $\delta = 1.5$  MeV<sup>27</sup>]. For the higher residual energy region, the slope value is the same as given by the analysis with unshifted  $U$ ; for the lower-energy region, it is roughly one unit smaller, and this applies for both nuclei.

The different approaches for evaluating  $\tau_n$  do not modify the previous remarks and they yield in fact the same  $n_I$  values. This conclusion underlines the importance of exciton state density in the shape of the distribution of the kinetic energy. Actually, the slope analysis is basically dependent on the accuracy of the functional form (8) obtained

from the constant spacing model. This point has been discussed by Bohning<sup>28</sup> and Williams,<sup>25</sup> who have concluded that the analytical form is a quite poor approximation only when  $U$  is small. The comparison made by Williams, Mignerey, and Blann<sup>29</sup> of the approximation (8) with some direct numerical values computed for the density of states generated by combinations of Nilsson orbitals yields fairly large discrepancies only for low  $U$  and near the closed shells. On the contrary, from real levels of a few nuclei, Grimes *et al.*<sup>30</sup> have found the expression in  $U^{m-1}$  to be a good approximation even at low excitation energy. At

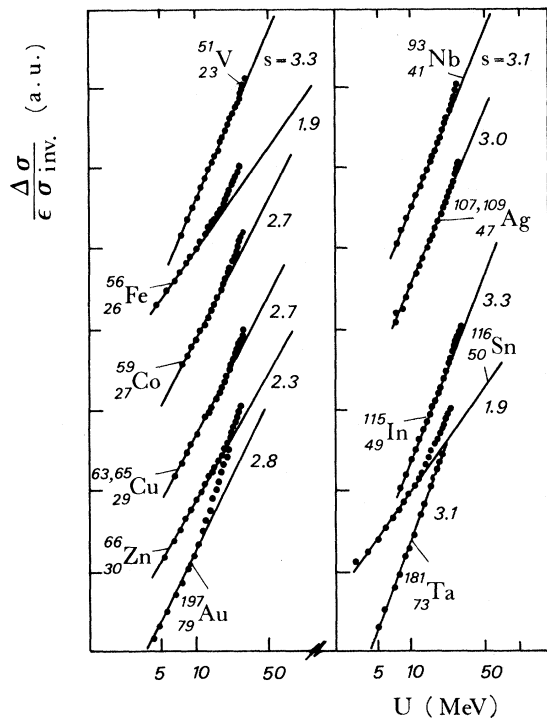


FIG. 7. Plots versus  $U$  for  $(\alpha, p)$  spectra with some couples of neighboring targets: evidence of an energy gap between the excitation of even-even nuclei and odd-odd or odd- $A$  nuclei. The slope analyses are also recalled.

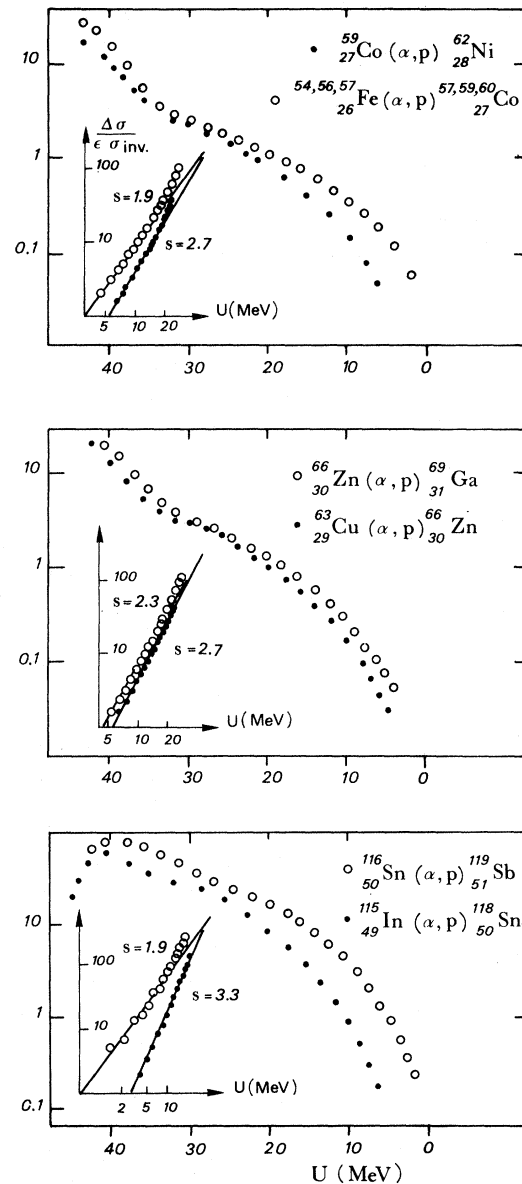


FIG. 8. Results of slope analysis for all studied  $(\alpha, p)$  reactions. Plots at  $30^\circ$  angle with the exciton method.

any rate, for the present ( $\alpha, p$ ) reactions, very low-lying states are not excited (see Figs. 6–8). By considering the region of residual energy analyzed here, and as the majority of the studied nuclei are far from closed shells, the use of the uniform-spacing model approximation seems to be quite justified.

The results of the slope analysis with unshifted energies and by means of the expression (8) for exciton state density show evidence for an odd-even effect: As listed in Fig. 7 and Table II, odd- $Z$  targets require  $n_I = 5$  and even  $Z$ ,  $n_I = 4$ . Until now, most of the ( $\alpha, p$ ) reactions have been investigated for odd- $Z$  nuclei and precompound analyses actually yielded  $n_I = 5$ .<sup>5</sup> A few results with even  $Z$  have reported  $n_I = 4$  for 30-MeV data with <sup>58</sup>Ni and <sup>124</sup>Sn<sup>5</sup> and 42 MeV with <sup>58</sup>Ni<sup>5</sup> and <sup>116</sup>Sn.<sup>21</sup> In this work this last trend is firmly established for <sup>54,56,57</sup>Fe, <sup>66</sup>Zn, and <sup>116</sup>Sn targets.

This odd-even effect is manifested by the intermediary of the residual energy. As shown in detail by Fig. 8, for a nearly identical kinetic spectrum of protons the energy of the levels excited in ( $\alpha, p$ ) emission is much lower for odd- $A$  and odd-odd residual nuclei (<sup>119</sup>Sb, <sup>57,59,60</sup>Co) than for even-even nuclei (<sup>60</sup>Ni, <sup>118</sup>Sn). The difference may exceed 3 MeV. The  $Q$  values cannot explain the result, since for the reactions with the three <sup>54,56,57</sup>Fe isotopes the  $Q$  values differ up to 2 MeV, and nevertheless the plots of the spectra against  $U$  are merged and interpreted by the same  $n_I$  number. In other terms, the even-even nuclei require higher energy to be excited. This gap is quite consistent with a pairing effect. The spectral data for these nuclei are then interpreted by larger  $n_I$  values. The same trend may be observed in ( $\alpha, n$ ) reactions<sup>31</sup>: The <sup>57</sup>Fe( $\alpha, n$ ), <sup>117</sup>Sn( $\alpha, n$ ), and <sup>119</sup>Sn( $\alpha, n$ ) lead to even-even nuclei and are fitted, respectively, by  $n_I = 5, 5$ , and  $4$ , while the ( $\alpha, n$ ) reactions leading to different parity nuclei are interpreted by  $n_I = 3$  and  $4$ . This odd-even feature is not so obvious in (<sup>3</sup>He,  $n$ ) reactions<sup>30</sup> and it cannot be observed in (<sup>3</sup>He,  $p$ ) or ( $p, n$ ) reactions where even-even nuclei can be reached from only odd-odd targets. For ( $p, n$ ) reactions, odd-even effects have been demonstrated; however, no general trend is observed.<sup>24,32</sup>

Now, if some pairing correction has to be introduced for evaluating the residual energy, one must first examine the form of the intermediate state density to be used in connection with shifted energy. The effect of pairing inclusion in the exciton state density has been investigated by Grimes *et al.*<sup>32</sup>; with shifted energies, the results from a Nilsson calculation<sup>29</sup> are fitted by a power one unit larger (or even greater near the closed shells) than expression (8), i.e.,  $U^n$  instead of

$U^{n-1}$ . According to that result, the slope of the plots with pairing correction is now  $n_I - 1$ . The analysis with pairing term will not change the  $n_I$  value if we take into account only the lower residual energy region; otherwise, for the higher region, a number larger by one unit is obtained. However it remains that such a conclusion giving two exciton numbers differing by one unit and characterizing a same reaction cannot be easily explained by assuming two-body internal transitions. The calculated contribution of precompound emission of a second proton for this emission energy range is too small in comparison with the first proton emission to be taken into account.

It may be noted that in analyses of nuclear reactions with the statistical theory another alternative for correcting energy is the back-shifted Fermi-gas model; the zero of the energy scale is taken now for even-even nuclei.<sup>33</sup> Unhappily, no expression of the exciton density state has been investigated for this procedure. Thus, the approximation (8) has to be assumed to remain valid. Then the analysis of the ( $\alpha, p$ ) reactions with an odd- $Z$  target is identical to the previous one with uncorrected energy, since the residual nucleus is even even. For even- $Z$  targets, the analysis with the residual energy shifted towards higher energy will raise the  $n_I$  value:  $n_I = 5$  for odd-even residual nucleus (see Fig. 6). The odd-odd residual nuclei would require even a higher  $n_I$ , for example, with the <sup>57</sup>Fe( $\alpha, p$ )<sup>60</sup>Co reaction.

The present discussion shows the importance of evaluating the energy in the exciton state density expression. More information about this problem is highly desirable. For the study here, we may conclude that no pairing correction of the

TABLE II. Results of the determination of the parameter  $n_I$  for 54.8-MeV ( $\alpha, p$ ) reactions. The even-even residual nuclei require the  $n_I$  value to be one unit larger than the other nuclei.

Reaction	Odd-even character of the residual nucleus	Slope $s$	$n_I$
<sup>51</sup> V( $\alpha, p$ )	even-even	3.3	5
<sup>54</sup> Fe( $\alpha, p$ )	odd-even	1.9	4
<sup>56</sup> Fe( $\alpha, p$ )	odd-even	1.9	4
<sup>57</sup> Fe( $\alpha, p$ )	odd-odd	1.9	4
<sup>59</sup> Co( $\alpha, p$ )	even-even	2.7	5
<sup>63,65</sup> Cu( $\alpha, p$ )	even-even	2.7	5
<sup>66</sup> Zn( $\alpha, p$ )	odd-even	2.3	4
<sup>93</sup> Nb( $\alpha, p$ )	even-even	3.5	5
<sup>107,109</sup> Ag( $\alpha, p$ )	even-even	3	5
<sup>115</sup> In( $\alpha, p$ )	even-even	3	5
<sup>116</sup> Sn( $\alpha, p$ )	odd-even	1.9	4
<sup>181</sup> Ta( $\alpha, p$ )	even-even	3.1	5
<sup>197</sup> Au( $\alpha, p$ )	even-even	2.8	5

energy seems to be appropriate for interpreting 54.8-MeV ( $\alpha, p$ ) reactions. This conclusion is consistent with the next quantitative analysis of the cross section. At the present stage of the question, we prefer to state that pairing effects are manifested through the difference of  $n_I$  values given by the analysis with unshifted energies according to the parity of the proton number of the target. A point of view from the reaction mechanism has been adopted by Griffin<sup>14, 24</sup> for discussing the odd-even effects in precompound reactions. With such an analysis, it can be said that for ( $\alpha, p$ ) reactions with an odd proton number target, the extra proton participates with the four nucleons of the diluted incident  $\alpha$  particle for dissipating the excitation energy. Thus, the initial configuration with  $n_I = 5$  is a  $3p-2n-0h$  state and with  $n_I = 4$ , a  $2p-2n-0h$  state.

#### B. Cross Sections

This last section will deal with the comparison between the experimental integrated cross sections and the different calculations of pre-equilibrium theory. Such formulations require the estimation of the transition probability  $\lambda_{n+2}$ .

In the expression for  $\lambda_{n+2}(\epsilon)$  of the hybrid model,<sup>7</sup> Blann uses values computed by Kikuchi and Kawai<sup>34</sup> for evaluating the mean free path of nucleons inside the nuclear matter. These values have been found consistent<sup>20</sup> with results from the optical

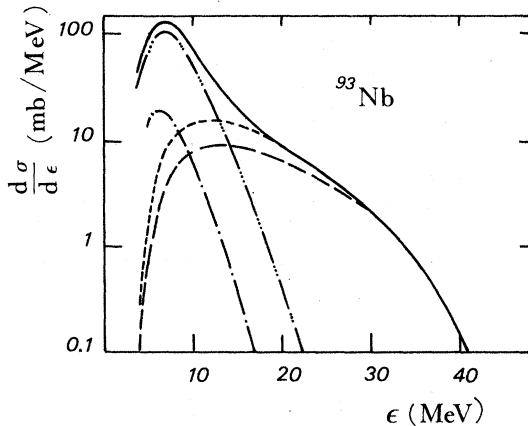


FIG. 9. The different calculated contributions for the proton emission induced by 54.8-MeV  $\alpha$  particles on  $^{93}\text{Nb}$ . The curve (—) is the total theoretical spectrum; the curve (---) is the precompound contribution for the initial configuration:  $n_I = 3p-2n-0h$ ; the curve (- - - -) is the total precompound emission; the curve (— — —) is the evaporation spectrum from the final nuclei after precompound emission; and the curve (.....) is the evaporation spectrum from the compound nucleus at equilibrium when no precompound emission has occurred.

model.<sup>35, 36</sup> Initially, Blann and Mignerey<sup>15</sup> have taken the reciprocal of  $\lambda_{n+2}$  as the exciton state lifetimes  $\tau_n$  to be used then for calculating absolute exciton model spectra.<sup>29</sup> Characteristic magnitudes for  $\lambda_{n+2}(\epsilon)$  are  $(2.5 \times 10^{22}) \text{ s}^{-1}$  and  $(4.5 \times 10^{22}) \text{ s}^{-1}$  according to  $\epsilon = 20$  and 40 MeV. It is useful to compare these results with calculations given by Harp and Miller<sup>8</sup> from the resolution of the master equations for the equilibration process inside a two-fermion gas by nucleon-nucleon collisions. Values extracted in this way are dependent on  $n$  and  $E$ . For 18-MeV protons bombarding  $^{181}\text{Ta}$ , these authors have found  $\lambda_{n+2}(E, n)$  equal approximately to  $(2 \times 10^{22}) \text{ s}^{-1}$  for  $n = 4$ . Another estimation, formally similar, due to Braga-Marcazzan *et al.*,<sup>11</sup> yields values of the same order of magnitude. With the exciton model formulation, we shall use for  $\lambda_{n+2}(n, E)$  values derived from  $\bar{\lambda}_{n+2}(1, E)$  estimated by Birattari *et al.*<sup>10</sup> according to the relation:

$$\lambda_{n+2}(n, E) = \bar{\lambda}_{n+2}(1, E) \frac{2}{n+1}.$$

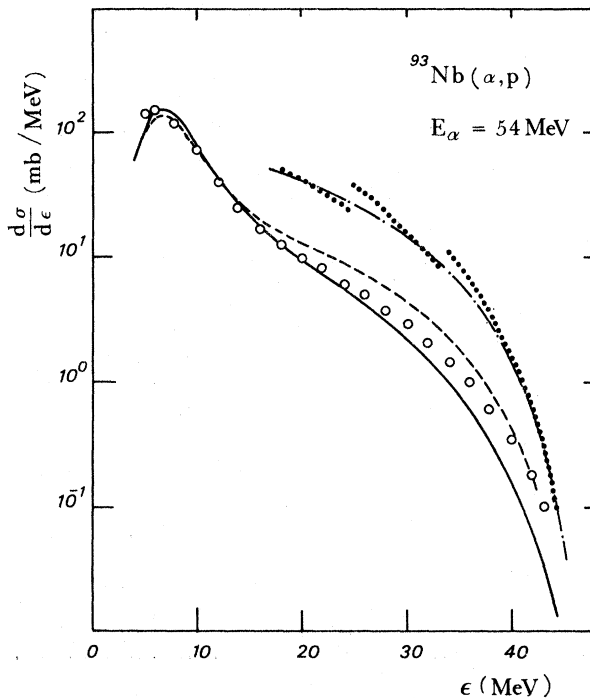


FIG. 10. The comparison of the experimental cross sections (O) for the 54.8-MeV  $^{93}\text{Nb}(\alpha, p)$  reaction with the results of the different calculations. The curve (—) represents the hybrid model (Ref. 7); the curve (---) represents the exciton model (Ref. 9); the curve (- - - -) represents the Griffin's model (Ref. 24); and the smooth averaging of the  $l$  sum in this last formulation is represented by the curve (.....). All the calculations have been performed for  $n_I = 5$  and with *a priori* fixed parameters.

For instance, with  $^{93}\text{Nb}(\alpha, p)$  reactions at 54.8 MeV the numerical value with  $n_I = 5$  is  $(2 \times 10^{22}) \text{s}^{-1}$ .

The total proton spectrum from  $(\alpha, p)$  reactions is computed according to the following scheme:

- (i) First, the precompound emission probability is computed from the composite system  $(N, Z)$  with energy  $E$  for only the first nucleon with  $n$  varying from  $n_I$  to  $n_{\text{eq}} = \sqrt{gE}$  by a step of 2.
- (ii) Then, for the residual nuclei  $(N-1, 2)$  and  $(N, Z-1)$  with energy  $U$  populated by this nucleon pre-equilibrium emission, an evaporation calculation for nucleons and  $\alpha$  particles is applied.
- (iii) Finally, the last stage computes the de-excitation of the compound nucleus at equilibrium

which is obtained with a probability equal to

$$1 - \sum_{\text{neutrons}} \sum_{\text{protons}} \sum_{n_I-2}^{n_{\text{eq}}} P_{n-2}.$$

The sum of these contributions multiplied by the cross section of capture of the  $\alpha$  particle obtained with an optical-model code<sup>37</sup> yields the total proton spectrum. A sample calculation is given in Fig. 9 where the pre-equilibrium contribution is computed according to the hybrid model. In this example, the contribution of the first precompound emission is also plotted in order to show its dominance. The importance of

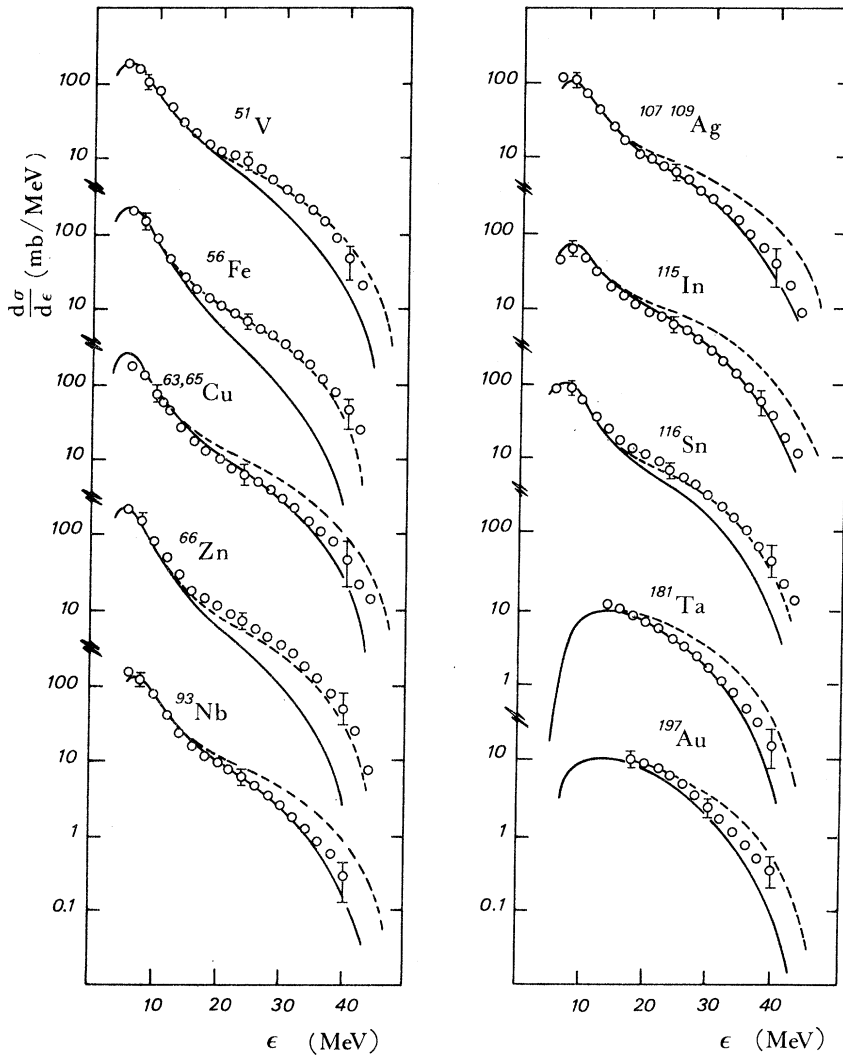


FIG. 11. Comparison of the experimental data ( $\circ$ ) with the hybrid model (Ref. 7) results for all the studied 54.8-MeV  $(\alpha, p)$  reactions. Each spectrum has its cross-section scale shifted from the preceding one by two decades. The calculations were performed with unshifted energies and with the nucleon mean free paths given by Kikuchi and Kawai (Ref. 34). The odd- $Z$  target reactions are interpreted by an initial exciton state  $n_I = 5$  (curves —), and even  $Z$  by  $n_I = 4$  (curves - - -).

the deexcitation of the residual nuclei  $(N, Z - 1, U)$  and  $(N - 1, Z, U)$  should be noted also [stage (ii)]: It contributes about 20% of the total evaporation process.

The compound-nucleus calculations were performed classically with Fermi-gas parameters:  $a = \frac{1}{8}A$  and level density of the exponential form  $U^{-2} \exp 2\sqrt{aU}$ , with pairing correction.

Figure 10 compares an experimental  $^{93}\text{Nb}(\alpha, p)$  spectrum with calculations of exciton and hybrid models. The different parameters have been already specified; as given by the slope analysis, the  $n_l$  configuration is built with  $3p-2n-0h$ . For energy calculations only, the exclusion principle correction is added without pairing term.

For comparison, it was useful to perform a calculation according to an expression by Lee and Griffin<sup>24</sup> which we recall here without further discussion:

$$P_n(\epsilon) = \sum_{l=0}^{l_{\max}} \frac{\rho(\pi_p - 1, \pi_n, \nu_p, \nu_n, U)}{\rho(\pi_p, \pi_n, \nu_p, \nu_n, E)} 2 \frac{2l+1}{\pi} \left( \frac{2m}{\hbar\epsilon} \right)^{1/2} \langle R_l^2 \rangle,$$

where  $\langle R_l^2 \rangle$  is a ratio where the numerator is the average square matrix element of transition between two states, the initial one is bound, and the final one has a proton in continuum with orbital angular momentum  $l$ . The denominator corresponds to internal transitions between bound states.

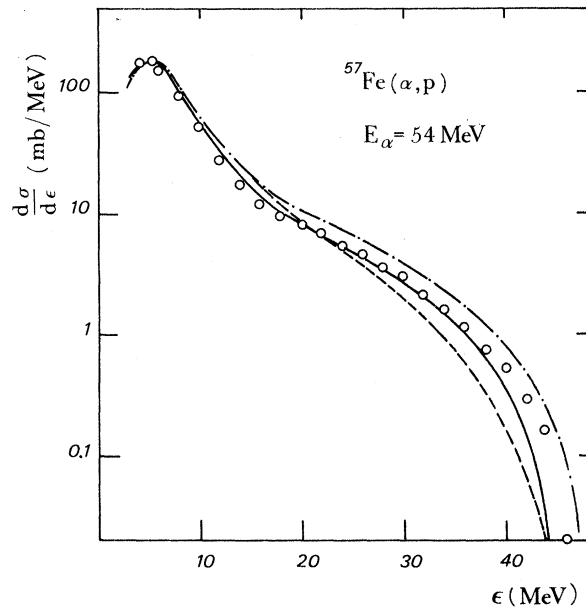


FIG. 12. The  $^{57}\text{Fe}(\alpha, p)^{60}\text{Co}$  cross sections (the experimental points are denoted by open circles,  $\circ$ ) are better interpreted by a hybrid calculation with  $n_l = 4$  and unshifted energy (curve —) than with  $n_l = 5$  and back-shifted energy (curve - - -). The result of a hybrid calculation with  $n_l = 4$  and back-shifted energy (curve - · -) is also shown.

This ratio is approximated as:

$$\langle R_l^2 \rangle = \frac{1}{2} r (k_c r)^2 [j_l(k_c r)]^2 + [\eta_l(k_c r)]^2,$$

where  $r$  is the nuclear radius equal to  $1.2A^{1/3}$  and  $k_c$  the proton wave number.  $j_l$  and  $\eta_l$  are the spherical Bessel functions. The summation is over all the  $l$  removed by the emission: This truncation with integer value of  $l_{\max}$  is responsible for the discontinuity in calculated values which can be removed by a smooth averaging of the  $l$  sum.<sup>24</sup>

As predicted by our previous discussion, the different theoretical shapes are quite concordant with the experimental spectrum. The last formula is somewhat higher than the two others which are in quantitative agreement with the experiment. The fit is equally good for the evaporation and pre-equilibrium components of the spectra. In the estimation of  $\tau_n$  the leading term is  $\lambda_{n+2}$ , and since for this quantity two approaches use values of the same order of magnitude, it is not surprising that both calculated cross sections are nearly identical. The values employed here for  $\lambda_{n+2}$  are quite realistic and correspond to mean free paths computed by Kikuchi and Kawai.<sup>34</sup> Thus, in the following series of Fig. 11 we com-

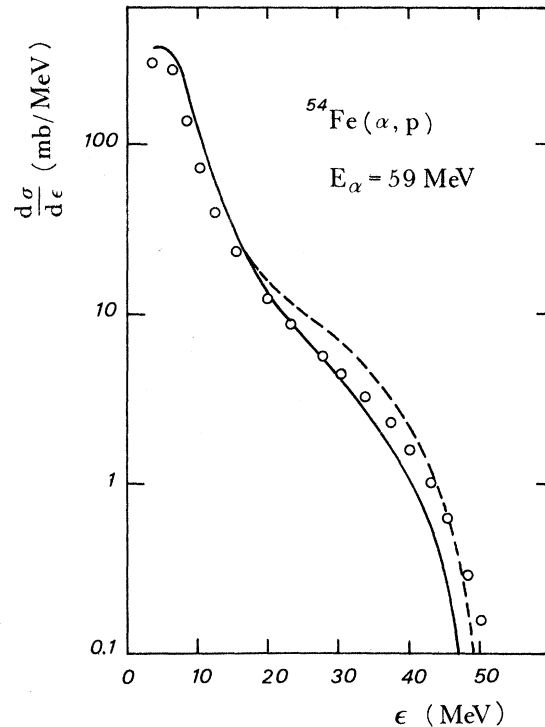


FIG. 13. Same as Fig. 10 for  $^{54}\text{Fe}(\alpha, p)$  reaction at 59 MeV, except that the calculations are carried with  $n_l = 4$ . The experimental data are due to Bertrand and Peele (Ref. 13).

pare the experimental spectra with only hybrid formulation, assuming that the exciton model leads to the same conclusion. The results of this interpretation of the absolute cross sections are consistent with the conclusion of the last section analysis of the spectrum shape. The whole set of the reported  $(\alpha, p)$  reactions are well interpreted by expressing the energy without pairing or back-shift correction and by taking  $n_I = 5$  or 4 according to the odd-even parity of the target atomic number. Another alternative for these conditions may be possible: Hybrid calculations with  $n_I = 4$  can also interpret the  $(\alpha, p)$  reactions with odd- $Z$  targets when the energy is shifted by a pairing correction and when an exciton state density of the form  $U^{n-1}$  is used. If a  $U^n$  form in this case seems to be more appropriate as found by Grimes *et al.*,<sup>32</sup> a more appropriate value for  $n_I$  will be 5. However, such absolute cross-section calculations do not follow the conclusion of the previous slope analysis which yields more acutely the  $n_I$  value. The back-shifted energy procedure in the cross-section computation leads also to some inconsistency with the slope analysis; for instance, the  $^{57}\text{Fe}(\alpha, p)^{60}\text{Co}$  is not fitted by a calculation with  $n_I = 5$  or more as suggested by the shape analysis. Actually, this reaction is quite well interpreted by  $n_I = 4$  when the energy is uncorrected (see Fig. 12).

With  $(\alpha, p)$  reactions at 54.8 MeV or higher energy [see Fig. 13 for the interpretation of

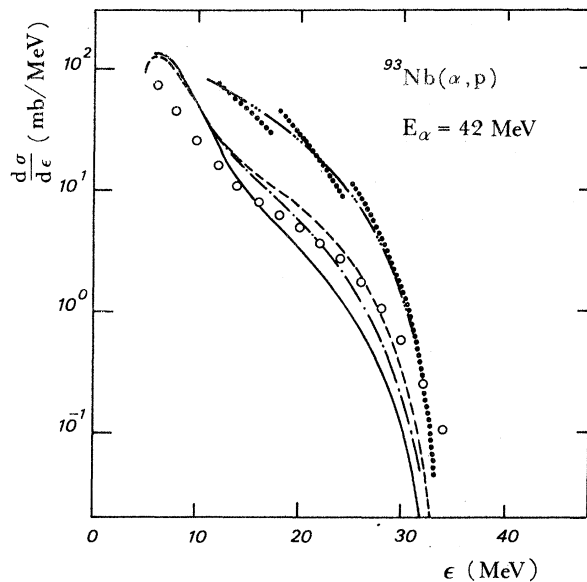


FIG. 14. Same as Fig. 10 for  $^{93}\text{Nb}(\alpha, p)$  reaction at 42 MeV. The experimental data are due to West (Ref. 17). A hybrid calculation performed with a value of mean free path 2 times larger than that calculated in Ref. 34 gives a better fit (curve — · — · —).

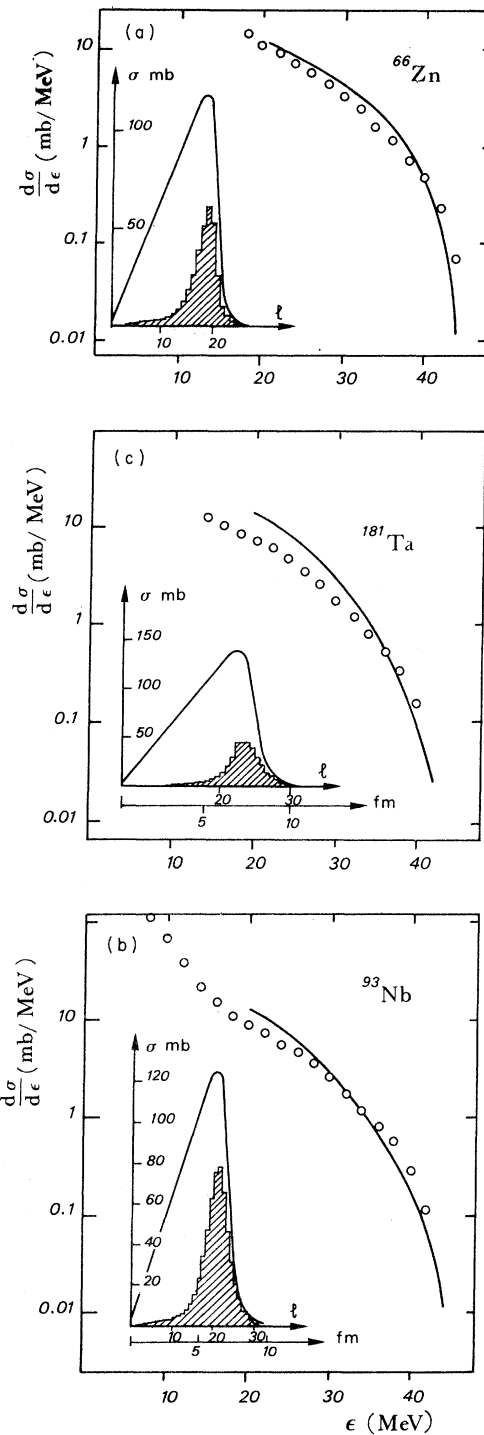


FIG. 15. (a)–(c) The results for the geometry-dependent hybrid formulation (Ref. 38) for a few 54.8-MeV  $(\alpha, p)$  spectra. In addition to the calculated curve (—) of the cross sections, the partial capture cross section (curve —) and the precompound proton emission for each partial zone (hatched surface) are also indicated in the inserted figure, versus the impact parameter.

$^{54}\text{Fe}(\alpha, p)$  data of Bertrand and Peele<sup>13</sup> at 59 MeV] the experimental results are in agreement with the theoretical predictions. However, significant discrepancies appear in proton-induced reactions,<sup>38</sup> in  $(\alpha, n)$  reactions,<sup>31</sup> or in  $(\alpha, p)$  reactions themselves at lower energies, as for instance in 42-MeV  $^{93}\text{Nb}(\alpha, p)$  reaction, the analysis of which is shown in Fig. 14. The disagreement may be due at low excitation energy to an underestimated evaporation calculation when no angular momentum effect is added. A more probable reason is that no geometrical factor is included in the precompound closed formulation even though it is a surface interaction.<sup>38</sup> In fact, mean-free-path values larger than preceding ones, generally by a factor of 2, give better agreement for  $(\alpha, n)$  reactions<sup>31</sup> or 42-MeV  $(\alpha, p)$  reactions (see Fig. 14).

The hybrid model allows inclusion of the reaction geometry dependence.<sup>38</sup> Thus, the consideration of nuclear matter distribution in the calculation of the internal transitions enhances the mean-free-path values at the diffuse edge of the nucleus. It gives then  $\tau_n$  values larger for nucleon escape. A second effect accompanying the nucleon density distribution is a geometrical dependence of the  $g$  values and the exciton state density.<sup>38</sup> However, the  $g$  variation according to the nuclear radius<sup>38</sup> leads to unrealistic values unexplained if we consider that  $g$  is a property of the potential created by all the nucleons, and, besides, the importance of this effect in cross section is weak. The exciton state density in the philosophy of our analysis is a result extracted from the experimental data and in fact the  $n_i$  numbers used ( $2p$  or  $3p-2n-0h$ ) implicitly assume that holes do not participate as a degree of freedom in sharing the excitation energy. This is consistent with a relative difficulty of creating very deep hole states.

Consequently, we shall use the following expression for the different partial zones:

$$\sigma_p(\epsilon) = \pi\chi^2 \sum_{l=0}^{\infty} (2l+1)T_l P_p(\epsilon, l),$$

where  $\pi\chi^2(2l+1)T_l$  is the capture cross section of the incident particle with an impact parameter equal to  $l\chi$ , and  $P_p(\epsilon, l)$  has a dependence on the Fermi-Thomas density distribution according to

$$P_p(\epsilon, l) = \frac{\rho(\pi_p - 1, \pi_p, \nu_p, \nu_n, U)}{\rho(\pi_p, \pi_n, \nu_p, \nu_n, E)} g_p \frac{\lambda_c(\epsilon, l)}{\lambda_c(\epsilon, l) + \lambda_{n+2}(\epsilon, \lambda)}$$

with

$$\lambda_{n+2}(\epsilon, l) = \frac{\lambda_{n+2}(\epsilon)}{1 + e^{(R - R_c)/a}}$$

$R_c$  is equal to  $1.07A^{1/3}$  fm and diffuseness  $a = 0.55$

fm.

$$\lambda_c(\epsilon, l) = \frac{2S+1}{2\pi\hbar g_p} \sum_0^{l^p} (2l^p+1)T_l^p,$$

where  $l^p$  is the angular momentum of emitted proton and  $T_l^p$  the corresponding transmission coefficient.

The precompound emission has been computed with the above expressions for the  $n_i = 4$  or 5 exciton state only; the deexcitation of this first state is quite predominant. Results which appear in Figs. 15(a)–15(c) for reactions with  $^{66}\text{Zn}$ ,  $^{93}\text{Nb}$ , and  $^{181}\text{Ta}$  are in good agreement with experiment.

In these figures, we can see that the major amount of precompound emission can be localized by this treatment in the nucleus periphery. On the contrary the central trajectories lead to the compound nucleus almost without any pre-equilibrium emission; this conclusion is consistent with results of the master equation for equilibrium nuclear relaxation.<sup>2</sup> Another distinction between the two processes can be pointed out in this geometry-dependent formulation. For precompound emission the times used for relating  $\tau_n$  are  $> (2 \times 10^{-22})$  s; these values are acceptable for intermediate states since they are a little longer than the transit time of a nucleon through the nucleus. The  $\tau_n$  values for central impacts are considerably shorter, about a few times  $10^{-23}$  s; the reason is naturally the dense nuclear matter involved in the calculations. If we suppose that the equilibrium is attained within a few collisions (2), the equilibrium time assumed by the model is typically  $< 10^{-22}$  s. The long lifetime compound nucleus is then obtained in a very short time. This idea is consistent with the statistical theory.

## V. CONCLUSION

The pre-equilibrium formulations have been shown to interpret with a fairly good success 54.8-MeV  $(\alpha, p)$  reactions either in the analysis of the proton spectrum shapes or in the analysis of the absolute cross sections; some insight into the reaction mechanism may also be considered by a geometry-dependent model. Both analyses have also demonstrated that precompound emission may be a possible way to investigate by the intermediary of exciton state density gross nuclear structure effects related to odd-even character of nucleus and pairing energy.

## ACKNOWLEDGMENTS

We would like to thank Professor M. Blann for having communicated to us some of his computer programs. We also would like to thank Professor E. Gadioli, Professor M. Lefort, Professor T. Magda, and Professor J. M. Miller for some valuable and stimulating discussions.

- <sup>1</sup>R. Serber, *Phys. Rev.* **72**, 1008 (1947).  
<sup>2</sup>G. D. Harp, J. M. Miller, and B. J. Berne, *Phys. Rev.* **165**, 1166 (1968).  
<sup>3</sup>J. J. Griffin, *Phys. Rev. Lett.* **17**, 478 (1966).  
<sup>4</sup>M. Blann, *Phys. Rev. Lett.* **21**, 1357 (1968).  
<sup>5</sup>C. K. Cline and M. Blann, *Nucl. Phys.* **A172**, 225 (1971).  
<sup>6</sup>F. C. Williams, *Phys. Lett.* **31B**, 184 (1970).  
<sup>7</sup>M. Blann, *Phys. Rev. Lett.* **27**, 333 (1971).  
<sup>8</sup>G. D. Harp and J. M. Miller, *Phys. Rev. C* **3**, 1847 (1971).  
<sup>9</sup>E. Gadioli, *Nuovo Cimento Lett.* **3**, 515 (1972).  
<sup>10</sup>C. Birattari, E. Gadioli, E. Gadioli-Erba, A. M. Grassi Strini, G. Strini, and G. Tagliaferri, *Nucl. Phys.* **A201**, 579 (1973).  
<sup>11</sup>G. M. Braga-Marcazzan, E. Gadioli-Erba, L. Milazzo-Colli, and P. G. Sona, *Phys. Rev. C* **6**, 1398 (1972).  
<sup>12</sup>M. Blann and F. Lanzafame, *Nucl. Phys.* **A142**, 559 (1970); W. Bowman and M. Blann, *ibid.* **A131**, 513 (1969); R. Bimbot and Y. Lebeyec, *J. Phys. Radium* **32**, 243 (1971); A. Demeyer, R. Chéry, A. Chevarier, N. Chevarier, J. Tousset, and Tran Minh Duc, *J. Phys. (Paris)* **31**, 847 (1970); S. M. Grimes, J. D. Anderson, J. W. McClure, B. A. Pohl, and C. Wong, *Phys. Rev. C* **3**, 645 (1971); **4**, 607 (1971); E. Gadioli, I. Iori, N. Moiho, and L. Zetta, *ibid.* **4**, 1412 (1971).  
<sup>13</sup>F. E. Bertrand and R. W. Peele, ORNL Report No. ORNL-4694, 1971 (unpublished).  
<sup>14</sup>J. J. Griffin, *Phys. Lett.* **24B**, 5 (1967).  
<sup>15</sup>M. Blann and A. Mignerey, *Nucl. Phys.* **A186**, 245 (1972).  
<sup>16</sup>L. W. Swenson and C. R. Gruhn, *Phys. Rev.* **146**, 886 (1966).  
<sup>17</sup>R. W. West, *Phys. Rev.* **141**, 1033 (1966).  
<sup>18</sup>N. P. Harvey and J. P. Bernou, *IEEE Trans. Nucl. Sci.* **NS-17**, 306 (1970).  
<sup>19</sup>F. S. Goulding, D. A. Landis, J. Cerny, and R. H. Pehl, *Nucl. Instrum. Methods* **27**, 1 (1964).  
<sup>20</sup>Tran Minh Duc, thesis, University of Lyon, 1972 (unpublished).  
<sup>21</sup>P. Pertosa, thesis, University of Lyon, 1971 (unpublished).  
<sup>22</sup>C. Hurwitz, S. J. Spencer, R. A. Esterlund, B. P. Pate, and J. B. Reynolds, *Nucl. Phys.* **54**, 65 (1964).  
<sup>23</sup>R. M. Eisberg, G. Igo, and H. E. Wegner, *Phys. Rev.* **100**, 1309 (1955).  
<sup>24</sup>E. V. Lee and J. J. Griffin, *Phys. Rev. C* **5**, 1713 (1972).  
<sup>25</sup>F. Williams, *Nucl. Phys.* **A133**, 33 (1969); **A166**, 231 (1971).  
<sup>26</sup>C. Birattari, E. Gadioli, A. M. Grassi-Strini, G. Strini, G. Tagliaferri, and L. Zetta, *Nucl. Phys.* **A166**, 605 (1971).  
<sup>27</sup>T. D. Newton, *Can. J. Phys.* **34**, 804 (1956).  
<sup>28</sup>M. Bohning, *Nucl. Phys.* **A152**, 529 (1970).  
<sup>29</sup>F. C. Williams, A. Mignerey, and M. Blann, to be published; M. Blann, in *Proceedings of the Fourth International School in Nuclear Physics, Rudziska, Poland, 1971*, edited by W. Zych (Warsaw U. P., Warsaw, Poland, 1971); and Autumn School in Nuclear Physics at Schleching, Germany, Report No. COO-3494-4, 1972 (unpublished).  
<sup>30</sup>S. M. Grimes, J. D. Anderson, J. W. McClure, B. A. Pohl, and C. Wong, *Phys. Rev. C* **5**, 830 (1972).  
<sup>31</sup>A. Alevra, R. Dumitrescu, I. R. Lukas, M. T. Magda, D. Plostinaru, E. Trutia, N. Chevarier, A. Chevarier, A. Demeyer, and Tran Minh Duc, *Nucl. Phys.* **A209**, 557 (1973).  
<sup>32</sup>S. M. Grimes, J. D. Anderson, J. W. McClure, B. A. Pohl, and C. Wong, *Phys. Rev. C* **7**, 343 (1973).  
<sup>33</sup>J. R. Huizenga, H. K. Vonach, A. A. Katsanos, A. J. Gorski, and C. J. Stephan, *Phys. Rev.* **182**, 1149 (1969).  
<sup>34</sup>K. Kikuchi and M. Kawai, *Nuclear Matter and Nuclear Reactions* (North-Holland, Amsterdam, 1968).  
<sup>35</sup>L. S. Rodberg, *Phys. Rev.* **124**, 210 (1961).  
<sup>36</sup>N. T. Porile, in *Nuclear Chemistry*, edited by L. Yaffe (Academic, New York, 1968), Vol. I, p. 57.  
<sup>37</sup>J. Raynal, code MAGALI, Saclay Report No. Saclay DPh. T/69-42, 1969 (unpublished).  
<sup>38</sup>M. Blann, *Phys. Rev. Lett.* **28**, 757 (1972).